IEEE Photonics Journal
An IEEE Photonics Society Publication

Open Access

A Chirped Subwavelength Grating With Both Reflection and Transmission Focusing

Volume 5, Number 2, April 2013

Xiaomin Lv
Weibin Qiu
Jia-Xian Wang
Yuhui Ma
Jing Zhao
Mengke Li
Hongyan Yu
Jiaoqing Pan

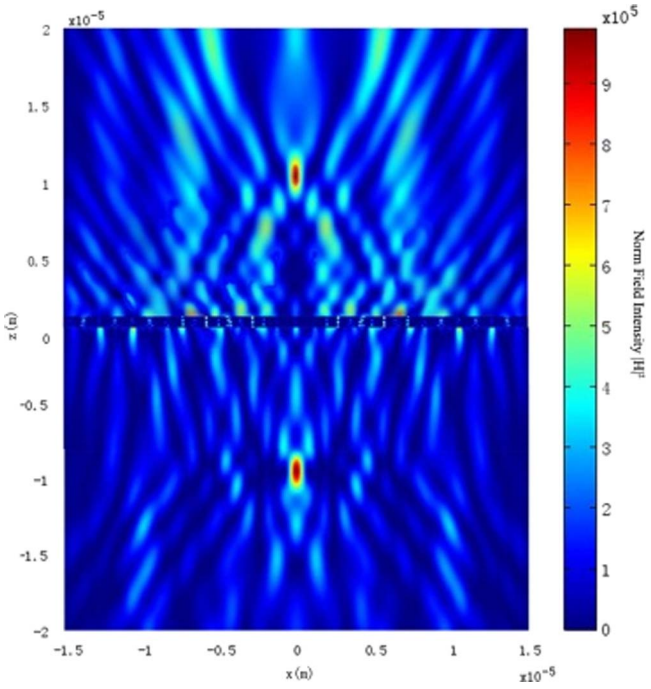

DOI: 10.1109/JPHOT.2013.2252333
1943-0655/$31.00 ©2013 IEEE

IEEE photonics SOCIETY

IEEE

A Chirped Subwavelength Grating With Both Reflection and Transmission Focusing

Xiaomin Lv,[1] Weibin Qiu,[1] Jia-Xian Wang,[1] Yuhui Ma,[1] Jing Zhao,[1] Mengke Li,[2] Hongyan Yu,[2] and Jiaoqing Pan[2]

[1]College of Information Science and Engineering, Huaqiao University, Xiamen 361021, China
[2]Institute of Semiconductors, Chinese Science Academy, Beijing 100083, China

DOI: 10.1109/JPHOT.2013.2252333
1943-0655/$31.00 ©2013 IEEE

Manuscript received February 26, 2013; revised March 7, 2013; accepted March 7, 2013. Date of publication March 15, 2013; date of current version April 3, 2013. This work was supported in part by the National Science and Technology Major Project under Grant 2011ZX02708, by the National 863 under Grant 2012AA012203, by the Opened Fund of the State Key Laboratory on Integrated Optoelectronics under Grant IOSKL2012KF12, and by the Natural Science Foundation of Fujian under Grant 2012J01277. Corresponding authors: W. Qiu and J.-X. Wang (e-mail: wbqiu@hqu.edu.cn; wangjx@hqu.edu.cn).

Abstract: A planar lens composed of a chirped subwavelength grating (CSG) structure with high numerical aperture (NA) was designed and analyzed in this paper. The reflectivity, transmission, and phase were calibrated as a function of the grating dimension using rigorous coupled wave analysis, while the focusing properties were numerically simulated by finite-element method. The designed CSG focused the reflected and transmitted waves that have approximately the same power ratios simultaneously. Numerical aperture values of the planar lens as high as 0.91 and 0.92 were obtained for normal incidence of TM and TE polarization light, respectively.

Index Terms: Subwavelength, grating, double focusing.

1. Introduction

With the development of microfabricating technology [1] and theoretical research, subwavelength gratings have got intensive attention to date. They are widely used as optical filters [2], [3], optical couplers [4]–[6], sensings [7], [8], and optical mirrors [9]–[13] for many unique characteristics.

Traditionally, distributed Bragg reflection (DBR) mirrors are composed of 20–40 dielectric stacks as both the top and bottom reflectors in order to obtain high reflectivity in vertical cavity surface emitting laser (VCSEL) [14], [15]. However, using high-contrast subwavelength grating can achieve high reflectivity with only a single dielectric layer as the top DBR mirror. It also shows less material absorption and mechanical losses. Metal mirrors have larger reflection bandwidths but lower reflectivity due to absorption loss. Dielectric mirrors can achieve a higher reflectivity but smaller bandwidth limited by small index difference. However, when subwavelength grating is used as mirrors, a very broad reflection spectrum and very high reflectivity can be achieved [12], [16]. In addition, subwavelength gratings are more compact and inexpensive than dielectric stacks in terms of fabrication and show good performance and long-term reliability. Similarly, they could also be used to replace the top dielectric stacks in microelectromechanical systems (MEMS) devices [17], [18].

In this paper, we proposed a chirped planar subwavelength grating to focus both the reflection and transmission beams that have approximately the same power ratio to the incident light. The total design procedure starts with calibrating the phase, transmission and reflectance distribution of the subwavelength grating with various dimensions. Then, the individual grating unit with certain

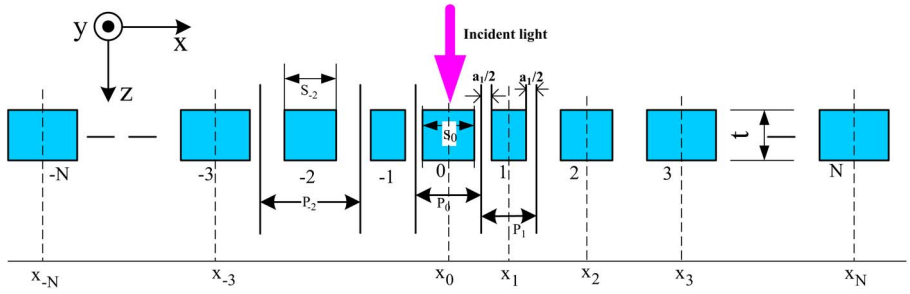

Fig. 1. Schematic of the CSG.

dimension distribution is collected to get the target phase distribution, which is similar to that of the Fresnel lens [19]. However, subwavelength gratings offer significant advantages over Fresnel lens, such as compact footprint, broadband, potential integration with other photonic devices, and focusing of both reflection and transmission with arbitrarily power ratios. The CSG focusing planar lens presented here offers new optical functionalities for a host of passive or active devices and is widely used as power splitter. Besides, with the subwavelength grating, the mode profile of a microlaser could be shaped directly through the output mirror, the expensive compound lens systems could be replaced in a series of consumer electronic products such as DVD players or digital cameras, and a cheaper alternative could be provided to the microlens arrays used in complementary metal–oxide–semiconductor (CMOS) and quantum computation implementations dependent on trapped atoms.

2. Theoretical Background

2.1. Calibration of the Reflection, Transmission, and Phase shift of the Periodic Subwavelength Grating

According to Snell's law, when the plane wave is normal incident upon the ordinary reflecting mirror, the reflected wave will go back in the same way without producing focusing effect. If the reflecting surface was replaced by a subwavelength grating, the plane wave shining on the grating will be reflected at an angle with respect to the normal of the grating. The phase distribution along the x-axis for each focusing element is [20]

$$\phi(x) = n\frac{\lambda}{2\pi}\left(\lambda - \sqrt{x^2 + f^2} + f\right) \tag{1}$$

where λ is the wavelength, f is the focal length, and n is the refractive index of the space in which the wave propagates. When $\phi(x)$ is more than 2π, it can be equivalent to the value between 0 and 2π. The phase shift ϕ_f of a subwavelength grating is given by dividing $\phi(x)$ with a modulus 2π [20]

$$\phi_f(x) = \phi(x) + 2m\pi \tag{2}$$

where m is an integer satisfying $0 \leq \phi_f \leq 2\pi$. This analysis method is equally applicable to the transmission wave.

2.2. Reflected and Transmitted Mechanism of CSG

The chirped subwavelength grating (CSG) is a single layer that consists of high-index and low-index materials shown in Fig. 1. The high-index material rods represented by blue rectangles are surrounded by low-index media. For simplicity of calculation, this paper uses air as low-index materials; similar results can be obtained in case of other materials.

In order to avoid the complicated and expensive grayscale lithography and etching techniques, the thickness (denoted as t) of the rods are kept constant in the design process. Since a grating period (denoted as P) consists of a piece of material rod (denoted as s) and airgap clearance

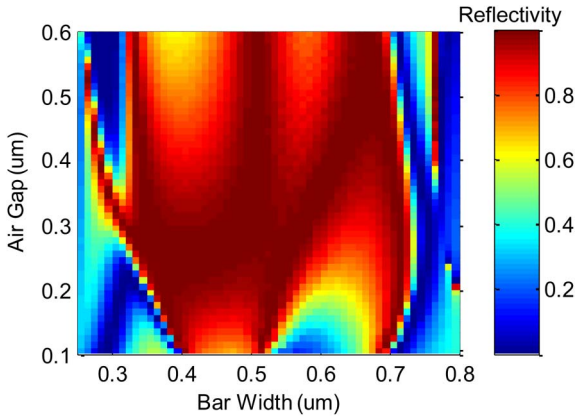

Fig. 2. Reflectivity contour as a function of rod width and airgap clearance for subwavelength grating.

(denoted as *a*), the complex reflection and transmission coefficient of the subwavelength grating can be calibrated as a function of rod width and airgap clearance. For a CSG, different rod widths and airgap clearances stand for various subwavelength grating rods (indexed as 0, ± 1, ± 2, etc., where 0 is the center bar). The left material rods have the same dimensions as the right for the symmetry. For a periodic subwavelength grating, the wavelength-dependent reflectance, transmittance, and phase shift of the grating can be easily obtained by using rigorous coupled wave analysis (RCWA) [21], as well as the relationship between reflection and transmission phase for a lossless symmetric system

$$\phi_r - \phi_t = \frac{\pi}{2} + m\pi \qquad m = 0, 1 \tag{3}$$

where ϕ_r and ϕ_t are the phase of reflection and transmission, respectively. Since the difference between ϕ_r and ϕ_t is either $\pi/2$ or $3\pi/2$, the phase distributions of the subwavelength grating on either side can be approximate the same with possible discontinuities with a phase jump of π.

It should be noted that, although the calculation of the reflection and transmission spectra and phase diagram is for periodic subwavelength gratings, it is also applicable to design a nonperiodic CSG focusing planar lens.

3. Design Process

The analysis above shows that both reflected and transmitted waves of the CSG are focused simultaneously if the phase shift distribution obeys (2). However, we also need the power distribution in certain applications. Therefore, the actual dimensions of subwavelength grating are chosen not only in accordance with phase path equation but also satisfying the particular power ratio. In this paper, we only design and analyze the reflection and transmission beams that have approximately the same power ratio, i.e., 50%, to the incident light. It is also applicable to design other planar lenses with respect to other power ratio.

3.1. Reflectivity and Phase of Periodic Subwavelength Grating

It is possible to calculate the complex reflection and transmission coefficients of any periodic structure and to numerically evaluate phase diagram, reflection, and transmission spectra for both transverse magnetic (TM) and transverse electric (TE) polarizations by using RCWA method. As an example, we considered CSG focusing planar lens design here for normal incidence of TM polarization (electric-field vector is parallel to the *x*-axis) light at a wavelength of 1.55 μm. The subwavelength grating thickness is fixed at 1.2 μm, while the airgap clearance changes from 0.1 μm to 0.6 μm and the rod width changes from 0.25 μm to 0.8 μm. Silicon is employed as the high-index material in this paper, and the refractive index is 3.48 at 1.55 μm. The reflection spectra and phase diagram can be obtained by using RCWA, as shown in Figs. 2 and 3, respectively. The refractive

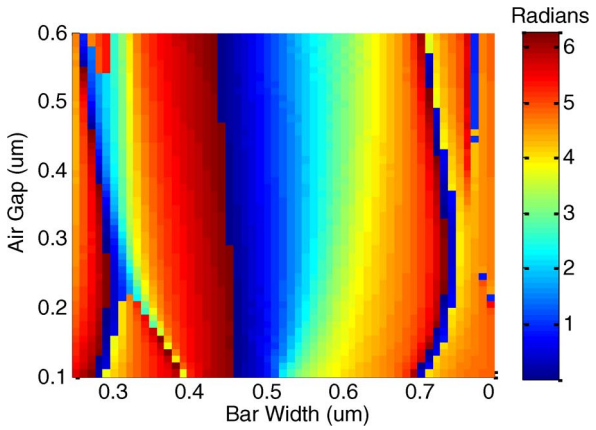

Fig. 3. Phase contour as a function of rod width and airgap clearance for subwavelength grating.

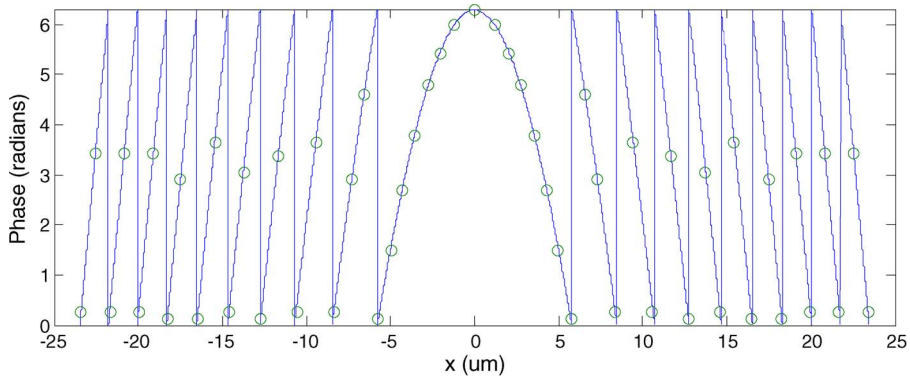

Fig. 4. Phase distribution of a CSG focusing planar lens. The blue curve is the ideal phase distribution with modulus 2π. Green circles are the phases of each material bar.

spectra and phase diagram for normal incidence of TE polarization (the electric field is parallel to the *y*-axis) light can be obtained by using the same method.

3.2. CSG Focusing Planar Lens

Given the focal length of 10 μm, the phase distribution can be calculated from (2), as shown in Fig. 4. The actual dimensions of periodic subwavelength grating are chosen, which satisfy the reflection and transmission beams that have approximately the same power ratio to the incident light at first. Then, the dimensions of CSG are selected with the phase path in accordance with (2). For a CSG, each period provides the desired phase with a certain rod width and airgap clearance (shown in the green circles in Fig. 4). Combining the subwavelength grating dimensions together is equivalent to using a discrete phase distribution to approximate the ideal distribution. Thus, double focusing planar lens with the same power ratio to reflected and transmitted waves is obtained by rational design of the subwavelength grating dimensions.

4. Simulation Results and Discussion

The performance of the focusing element is evaluated by using COMSOL finite-element method (FEM) numerical simulation. The plane wave of TM polarization normal incident from the positive *z* half-plane (close to the subwavelength grating surface) is approximately the same power ratio as the reflected and transmitted waves by the 46.4-μm-width CSG planar lens. The H-field intensity (normalized by incident field intensity) of both the reflection side and the transmission side is plotted

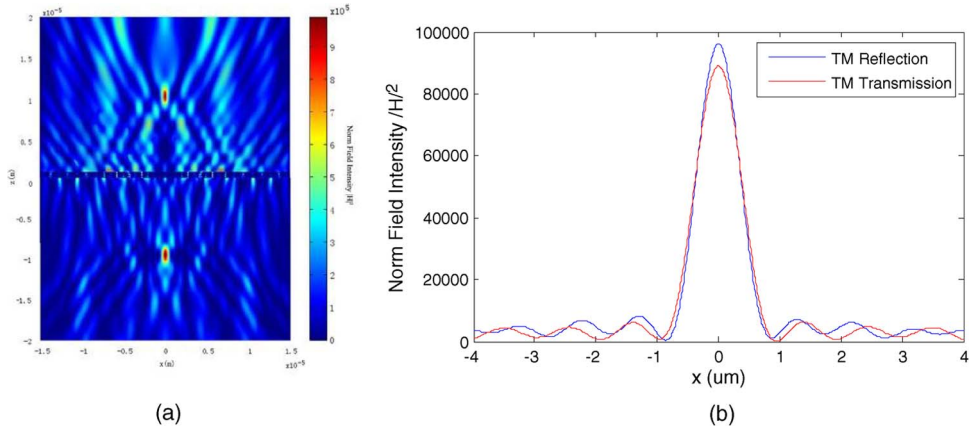

Fig. 5. (a) H-field intensity distribution of a CSG. (b) H-field intensity distribution at the reflection and transmission focal plane.

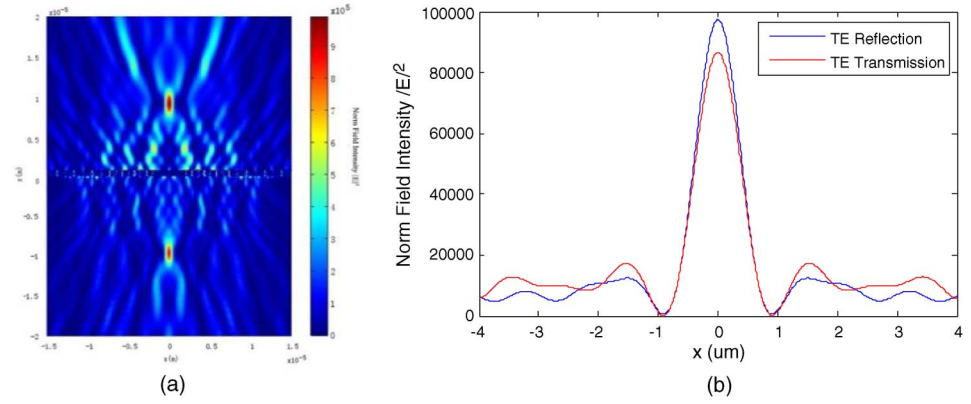

Fig. 6. (a) E-Field intensity distribution of a CSG. (b) E-field intensity distribution at the reflection and transmission focal plane.

in Fig. 5(a). The reflected beam is focused to a spot 10.7 μm above the CSG (close to the designed focal length of 10 μm), while the transmitted beam is focused at 10.5 μm below the CSG. Thus, the NA is 0.91. At the focal plane, the field distribution is shown in Fig. 5(b). The blue curve is H-field intensity of reflected wave, with a full-width half-maximum (FWHM) of 0.79 μm, which is close to the diffraction limit. The red curve is the H-field intensity of transmitted wave, with a FWHM of 0.86 μm.

For the TE polarization, we obtain similar results, where the power ratio to reflected and transmitted waves by the 49.2-μm-wide CSG planar lens is approximately the same. The E-field intensity on both the reflection side and the transmission side is plotted in Fig. 6(a). The reflected beam is focused to a spot 10.4 μm above the CSG, resulting in an NA is 0.92, and transmitted beam is focused to a spot 10.8 μm below the CSG. At the focal plane, the field distribution is shown in Fig. 6(b). The blue curve is E-field intensity of reflected wave, with a FWHM of 0.825 μm. The red curve is E-field intensity of transmitted wave. It has a FWHM of 0.85 μm.

When the plane wave incidences to the CSG at a tilted angle, the phase shift distribution of reflection and transmission waves no longer satisfies the focusing condition (2); hence, no focusing exists. We also investigated the wavelength dependence of the designed structure from 1.48 μm to 1.62 μm. The power ratio, the FWHM of the focused spot, and the focal distance for both the reflected and transmitted beams for both TE and TM versus wavelength for 1.48–1.62 μm are plotted in Fig. 7(a)–(c), respectively. The power ratio of the focused reflected and transmitted beams keeps almost the same, while the focus length deviates with the modification of wavelength. As a

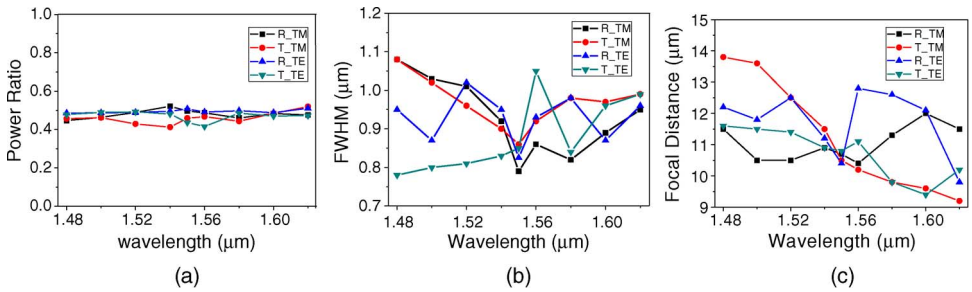

Fig. 7. (a) The power ratio, the FWHM of the focused spot, and the focal distance, for both the reflected and transmitted beams for both TE and TM versus wavelength for 1.48–1.62 μm (a) Power ratio. (b) FWHM of focused spot. (c) Focal distance.

result, high fabrication tolerance can be expected with the designed device due to the broadband wavelength property.

5. Conclusion

We have presented a high-numerical-aperture double-focusing planar lens composed of CSG. The focusing planar lens can be designed by calibrating the subwavelength grating dimensions to achieve a certain reflectivity, transmission, and phase distribution. The subwavelength grating dimensions have been chosen by two conditions; one is to make sure both the reflection and transmission beams have approximately the same power ratio to the incident light, and the other is that the phase path should meet focusing condition (2). By FEM numerical simulation, a high NA of 0.91 has been obtained for a CSG focusing planar lens in the condition that TM polarization incident light at a wavelength of 1.55 μm, while FWHMs of 0.79 μm and 0.86 μm have been achieved at the reflection and transmission focal planes, respectively. For the TE polarization light, an NA of 0.92 has been obtained, and the FWHMs are 0.825 μm and 0.85 μm at the reflection and transmission focal planes, respectively. We believe that our method can greatly reduce the cost of optical components while offering new application functionalities including active phase front correction, dynamic focusing, and cavity resonance tuning.

Acknowledgment

The authors are grateful to Prof. W. Wang, Prof. H. Zhu, and Prof. L. Zhao from Institute of Semiconductors, Chinese Academy of Science, and Prof. L. L. Goddard from University of Illinois at Urbana Champaign for their encouragement and productive discussions.

References

[1] J. R. Leger, M. G. Moharam, and T. K. Gaylord, "Diffractive optics: An introduction to the feature issue," *Appl. Opt.*, vol. 34, no. 14, pp. 2399–2400, May 1995.
[2] S. Tibuleac and R. Magnusson, "Reflection and transmission guided-mode resonance filters," *J. Opt. Soc. Amer. A*, vol. 14, no. 7, pp. 1617–1626, Jul. 1997.
[3] Y. Kanamori, T. Kitani, and K. Hane, "Guided-mode resonant grating filter fabricated on silicon-on-insulator substrate," *Jpn. J. Appl. Phys.*, vol. 45, no. 3A, pp. 1883–1885, Mar. 2006.
[4] P. Cheben, S. Janz, D.-X. Xu, B. Lamontagne, A. Delage, and S. Tanev, "A broad-band waveguide grating coupler with a subwavelength grating mirror," *IEEE Photon. Technol. Lett.*, vol. 18, no. 1, pp. 13–15, Jan. 2006.
[5] K. Kintaka, J. Nishii, Y. Imaoka, J. Ohmori, S. Ura, R. Satoh, and H. Nishihara, "A guided-mode-selective focusing grating coupler," *IEEE Photon. Technol. Lett.*, vol. 16, no. 2, pp. 512–514, Feb. 2004.
[6] Z. Cheng, X. Chen, C. Y. Wong, K. Xu, C. K. Y. Fung, Y. M. Chen, and H. K. Tsang, "Focusing subwavelength grating coupler for mid-infrared suspended membrane waveguide," *Opt. Lett.*, vol. 37, no. 7, pp. 1217–1219, Apr. 2012.
[7] R. Magnusson, Y. Ding, K. J. Lee, P. S. Priambodo, and D. Wawro, "Characteristics of resonant leaky mode biosensors," in *Proc. SPIE*, Nov. 2005, vol. 6008, pp. 1–10.
[8] D. Fattal, M. Sigalas, A. Pyayt, Z. Li, and R. G. Beausoleil, "Guided-mode resonance sensor with extended spatial sensitivity," in *Proc. SPIE*, Sep. 2007, vol. 6766, p. 67660J.
[9] Y. Hori, H. Asakura, F. Sogawa, M. Kato, and H. Serizawa, "External-cavity semiconductor laser with focusing grating mirror," *IEEE J. Quantum Electron.*, vol. 26, no. 10, pp. 1747–1755, Oct. 1990.

[10] S. Block, E. Gamet, and F. Pigeon, "Semiconductor laser with external resonant grating mirror," *IEEE J. Quantum Electron.*, vol. 41, no. 8, pp. 1049–1053, Aug. 2005.
[11] Y. Ding and R. Magnusson, "Use of nondegenerate resonant leaky modes to fashion diverse optical spectra," *Opt. Exp.*, vol. 12, no. 9, pp. 1885–1891, May 2004.
[12] C. F. R. Mateus, M. C. Y. Huang, L. Chen, C. J. Chang-Hasnain, and Y. Suzuki, "Broad-band mirror (1.12–1.62 μm) using a subwavelength grating," *IEEE Photon. Technol. Lett.*, vol. 16, no. 7, pp. 1676–1678, Jul. 2004.
[13] Y. Ding and R. Magnusson, "Resonant leaky-mode spectral-band engineering and device applications," *Opt. Exp.*, vol. 12, no. 23, pp. 5661–5674, Nov. 2004.
[14] M. C. Huang, Y. Zhou, and C. J. Chang-Hasnain, "A surface-emitting laser incorporating a high-index-contrast subwavelength grating," *Nat. Photon.*, vol. 1, no. 2, pp. 119–122, Feb. 2007.
[15] M. C. Y. Huang, Y. Zhou, and C. J. Chang-Hasnain, "Single mode high-contrast subwavelength grating vertical cavity surface emitting lasers," *Appl. Phys. Lett.*, vol. 92, no. 17, pp. 171108-1–171108-3, Apr. 2008.
[16] C. F. R. Mateus, M. C. Y. Huang, Y. Deng, A. R. Neureuther, and C. J. Chang-Hasnain, "Ultrabroadband mirror using low-index cladded subwavelength grating," *IEEE Photon. Technol. Lett.*, vol. 16, no. 2, pp. 518–520, Feb. 2004.
[17] W. Jung, S. Kim, and O. Solgaard, "High-reflectivity broadband photonic crystal mirror MEMS scanner scanner," in *Proc. IEEE 14th Int. Conf. Solid-State Sens., Actuators Microsyst.*, Lyon, France, Jun. 2007, pp. 1513–1516.
[18] W. Jung, S. Kim, and O. Solgaard, "High-reflectivity broadband photonic crystal mirror MEMS scanner with low dependence on incident angle and polarization," *J. Microelectromech. Syst.*, vol. 18, no. 4, pp. 924–932, Aug. 2009.
[19] T. Shiono and K. Setsune, "Blazed reflection micro-Fresnel lenses fabricated by electron-beam writing and dry development," *Opt. Lett.*, vol. 15, no. 1, pp. 84–86, Jan. 1990.
[20] T. Shiono, M. Kitagawa, K. Setsune, and T. Mitsuyu, "Reflection micro-Fresnel lenses and their use in an integrated focus sensor," *Appl. Opt.*, vol. 28, no. 16, pp. 3434–3442, Aug. 1989.
[21] M. G. Moharam and T. K. Gaylord, "Rigorous coupled-wave analysis of planar-grating diffraction," *Opt. Soc. Amer.*, vol. 71, no. 7, pp. 811–818, Jul. 1981.